

Original Research

Assessment of Influencing Factors of Nitrogen Dioxide in Shandong, China, Using the Geographical Detector Method

Huisheng Wu^{1*}, Yongheng Li¹, Maogui Hu²

¹College of Oceanography and Space Informatics, China University of Petroleum (East China), Qingdao, Shandong, 266580, China

²State Key Laboratory of Resources and Environmental Information System, Institute of Geographic Sciences and Natural Resources Research, CAS, Beijing 100101, China

Received: 25 July 2021

Accepted: 8 January 2022

Abstract

To realize a sustainable development strategy, it is important to explore the influencing factors of air pollutants. Daily monitoring data for nitrogen dioxide (NO₂) in Shandong Province from 2014 to 2019 were used in the geographical detectors to analyze the influencing factors. Through geographical detection, the action of influencing factors and their interactions on spatial heterogeneity were explored. The main influencing factors of NO₂ concentration were the daily temperature range and industrial smoke dust emissions, with *q* values of 0.4625 and 0.388, respectively, and the interaction effects of most influencing factors were characterized by bilinear enhancement. The interaction between urbanization rate and increases in secondary industry was the strongest, with an average 6-year *q* value of 0.716, followed by the interaction between the daily temperature range and increases in secondary industry, with a *q* value of 0.705. NO₂ air pollution was more severe in winter than in summer. The results indicate that we should take corresponding measures to control and reduce NO₂ air pollution based on the main influencing factors and their spatiotemporal characteristics.

Keywords: nitrogen dioxide, geographical detectors, influencing factors, spatiotemporal analysis

Introduction

Nitrogen dioxide (NO₂) plays an important role in the formation of ozone. Anthropogenic NO₂ mainly comes from high-temperature combustion processes, including those at fossil fuel power plants, petroleum refineries and metallurgical furnaces [1, 2]. NO₂ is

one of the main causes of acid rain [3, 4], which can affect competition between wetland and terrestrial plant species and composition changes, increased contents of NO₂ will cause atmospheric visibility reduction, surface water acidification, eutrophication, and increased amount of toxins harmful to fish and other aquatic organisms. Studies have shown that NO₂ is detrimental to human health [5, 6]. NO₂ stimulates the respiratory tract and lung mucosa, which can substantially damage lung function and increase the probability of respiratory infection [7, 8]. In addition, pathological studies have

*e-mail: wuhuisheng@upc.edu.cn

shown that NO_2 has an important correlation with deterioration of asthma [9, 10]. China's rapid economic development and urbanization have been accompanied by massive resource and energy consumption, leading to great increases in the emissions of NO_2 and other atmospheric pollutants [11].

Various influencing factors have different impacts on air pollutants, and social and economic factors, such as the number of civilian vehicles, have positive relationships with urban air pollution [12]. Additionally, most meteorological factors, such as average precipitation and average wind speed, are negatively correlated with air pollution [13]. Although an increasing number of studies have focused on the spatiotemporal patterns of air pollutants [14-16], there are still very few studies on the dependence and heterogeneity of air pollution patterns in time and space.

In this study, we considered the temporal and spatial distribution characteristics of NO_2 pollution and selected anthropogenic and meteorological factors to determine the influencing factors that had the strongest correlation with the spatial heterogeneity of NO_2 . The results are intended to provide information for the formulation of more effective air pollution mitigation measures and related policies.

Data

Study Area

Shandong Province is located on the eastern coast of China (Fig. 1) and covers an area of 158,000 square kilometers. Its terrain is complex, with mountains protruding in the central part, low-lying and flat terrain in the southwest and northwest, and gentle hills undulating in the east; the general terrain trend is characterized by a framework of mountains and hills and a crisscrossing plain basin. The annual average temperature is 11.0-14.7°C. The average annual precipitation is generally between 500 mm and 848 mm,

decreasing from southeast to northwest. Light resources are abundant, with an average annual illumination time of 2290-2890 hours. Shandong is the province with the third largest economy, with a regional GDP of 7106.75 billion yuan at the end of 2019.

Data Source

We obtained daily NO_2 concentration from January 1, 2014, to December 31, 2019, from the online air quality data website maintained by the China National Environmental Monitoring Center (<http://www.cnemc.cn/>). For each station, the daily NO_2 concentration was the 24-hour average values. The monthly concentration was calculated on the basis of daily values. The seasonal value was the average for the corresponding three months. The annual value was calculated from the sum of twelve-monthly concentration values. Ninety-one typical monitoring stations distributed in 16 cities of Shandong Province were selected (Fig. 1).

In view of the data availability and the correlations between the different influencing factors and NO_2 , ten influencing factors were selected. Daily temperature, precipitation and wind speed data were obtained from monitoring stations, and the data of daily temperature range was retrieved from the China Meteorological Data Network (<http://data.cma.cn>). We also obtained monthly data on the sunshine hours and yearly data on the urbanization rate, increases in secondary industry, industrial smoke and dust emissions, number of large trucks and number of civilian vehicles from the Shandong Provincial Bureau of Statistics.

Monthly, quarterly, and annual data for the influencing factors were used. In Shandong, spring includes March, April, and May; summer includes June, July, and August; autumn includes September, October, and November; and winter includes December, January, and February.

Through the statistical software R 3.6 and the package kernlab, the K value of each influencing factor was determined based on the elbow method.

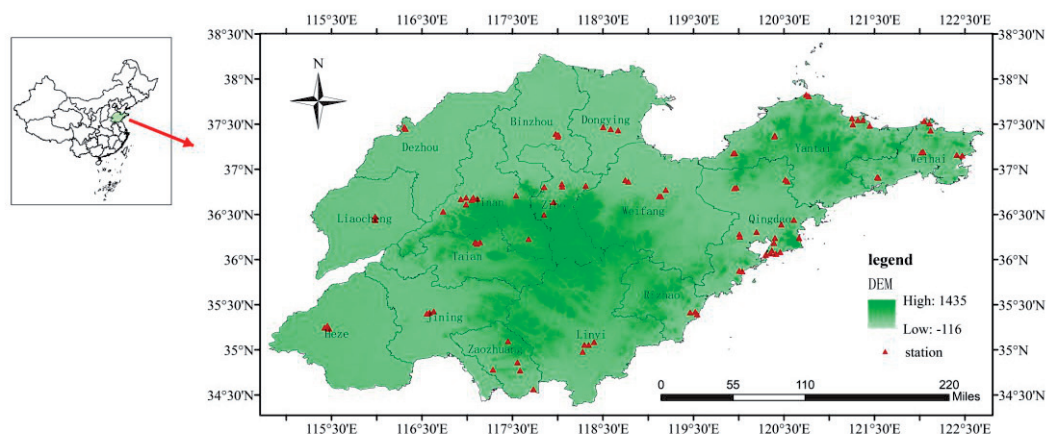


Fig. 1. Distribution of monitoring stations in Shandong Province.

We imported the K values into the geographical detectors and obtained the results.

Methods

Geographical detectors are a statistical method based on spatial differentiation. The method can be used to reveal the spatial similarity or correlation between a certain independent variable and related dependent variables. This method can address both numerical data and qualitative data, and it can explain whether two independent variables are linearly enhanced, nonlinearly enhanced or weakened by detecting the significance of their interaction; moreover, this method has no limitations compared to traditional statistical methods [17].

Factor Detector

To explore the spatial differentiation of dependent variables and probe into the explanatory power of the influencing variables, factor detection is performed by calculating the q value, and the corresponding expression is shown as Formula (1).

$$q = 1 - \frac{\sum_{h=1}^L N_h \sigma_h^2}{N \sigma^2} = 1 - \frac{SSW}{SST} \tag{1}$$

where q is the explanatory power of each influencing factor on NO₂. The range of q is from 0 to 1. The greater the value of q is, the stronger the explanatory power of the corresponding influencing factor on NO₂ is, and the higher the spatial correlation with NO₂ is. In the limit case, when the q value of an influencing factor is 1, it means that the factor fully explains the spatial difference in NO₂. In contrast, when the q value is 0, it means that the factor has no correlation.

Where h is the strata of factor X (h = 1, 2..., L), that is, the classification of risk factors for NO₂. N_h and N are the numbers of units in layer h and the whole region, respectively. σ_h² and σ² are the variances in NO₂ values for layer h and the whole region, respectively. SSW and SST represent the sum of intralayer variances and the total variance of the whole region, respectively.

Interaction Detector

To determine the interaction of two individual influencing factors on NO₂ in geographical space, the sum of q (X1) and q (X2), the interaction detection results of q(X1∩X2) and the maximum or the minimum value between q (X1) and q (X2) are compared to determine whether the interaction of the two factors increases or decreases the impact on NO₂ or whether the two factors work independently. The interactions can be divided into five categories including weakened,

nonlinear; weakened, single factor nonlinear; enhanced, double factors; independent; enhanced, nonlinear.

Ecological Detector

Ecological detection is used to assess whether there is a significant difference in the spatial distribution correlation between two factors affecting NO₂. The standard F-test used for the evaluation is shown in Formula (2):

$$F = \frac{N_{x1}(N_{x2} - 1)SSW_{x1}}{N_{x2}(N_{x1} - 1)SSW_{x2}} \tag{2}$$

$$SSW_{x1} = \sum_{h=1}^{L1} N_h \sigma_h^2 \tag{3}$$

$$SSW_{x2} = \sum_{h=1}^{L2} N_h \sigma_h^2 \tag{4}$$

where F is the test value, and N_{x1} and N_{x2} represent the sample sizes of the two factors. SSW_{x1} and SSW_{x2} represent the sum of the intralayer variances of the layers formed by the two factors. L₁ and L₂ represent the numbers of delamination of the two factors. The model null hypothesis H₀ is SSW_{x1} = SSW_{x2}; if H₀ is rejected at the significance level of 0.05, it indicates that there is a significant difference between the two factors, and the correlation value is “Y”; conversely, a correlation value “N” indicates that there is no significant difference [18].

Risk Detector

Risk detection compares the difference in average values among subregions using t statistics for testing; the corresponding equation is given in Formula (5):

$$t \frac{\bar{y}_{h=1} - \bar{y}_{h=2}}{[\frac{\text{Var}(\bar{Y}_{h=1})}{n_{h=1}} + \frac{\text{Var}(\bar{Y}_{h=2})}{n_{h=2}}]^{1/2}} = \frac{\bar{Y}_{h=1} - \bar{Y}_{h=2}}{[\frac{\text{Var}(\bar{Y}_{h=1})}{n_{h=1}} + \frac{\text{Var}(\bar{Y}_{h=2})}{n_{h=2}}]^{1/2}} \tag{5}$$

where Y_h represents the mean value of attributes in layer h where the factor is located; n_h is the number of samples in subregion h; and var indicates the variance.

Results

Factor Detection Results

Factor detection was performed by using the average value over six years; the q value of the daily temperature range was the highest, while the q value of the urbanization rate was the smallest. The factor detection results were shown in Fig. 2.

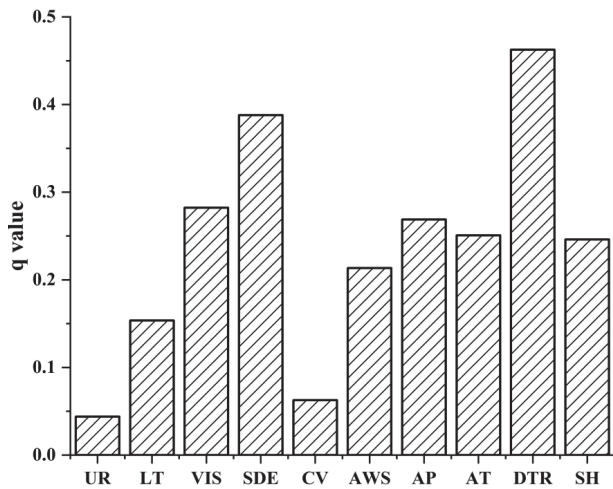


Fig. 2. Comparison chart of factor detection results.

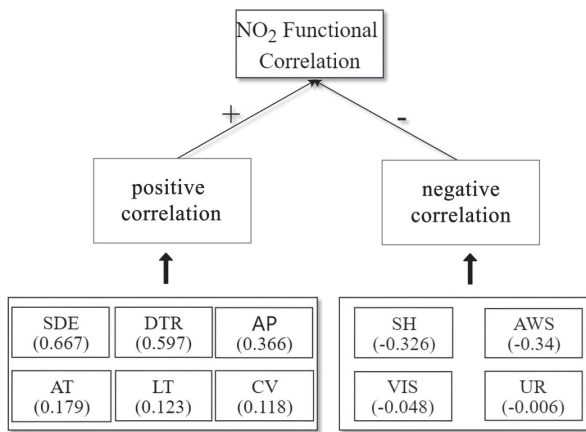


Fig. 3. Framework of positive and negative correlations.

On the basis of the obtained positive and negative correlations, we constructed the framework shown in Fig. 3. Spearman rank correlation analysis was used to judge the influence direction of the influencing factors on NO₂.

Interaction Detection Results

The interaction detection results were shown in Fig. 4. The values for seven groups exceeded 0.65, which were sequentially listed as follows: urbanization rate \cap increases in secondary industry (0.716), increases in secondary industry \cap daily temperature range (0.705), urbanization rate \cap daily temperature range (0.69), average temperature \cap industrial smoke dust emissions (0.659), number of large trucks \cap average temperature (0.655), increases in secondary industry \cap average wind speed (0.651), and increases in secondary industry \cap average temperature (0.65). The seven sets of data were characterized by bilinear enhancement. Among the combinations with interaction detection

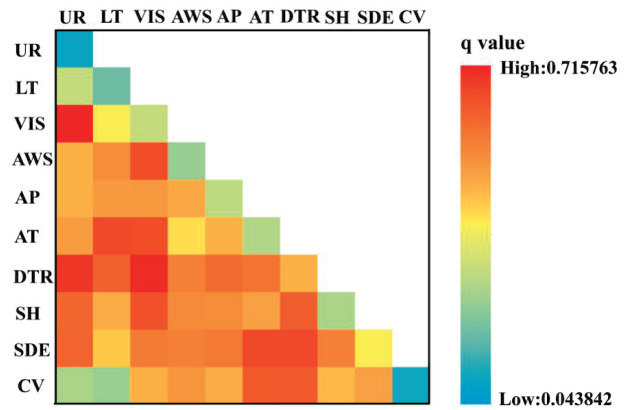


Fig. 4. Chart of interaction detection results.

values greater than 0.5, the number of industrial smoke dust emissions was seven, and the daily temperature range and urbanization rate accounted for six, which were consistent with the results obtained by factor detection.

Ecological Detection Results

We found that the differences among most influential factors were not statistically significant. However, there were significant differences between the daily temperature range and other influencing factors except industrial smoke dust emissions. The urbanization rate was significantly different from the increases in secondary industry and industrial smoke dust emissions. The differences between industrial smoke dust emissions and number of large trucks and between industrial smoke dust emissions and number of civilian vehicles were significant. Overall, there were significant differences in the spatial distribution correlation between the daily temperature range and other influencing factors affecting NO₂.

Risk Detection Results

The average values of NO₂ in all subregions were obtained. Specifically, we obtained the number of subregions by the K-means clustering method, and each subregion had a corresponding average value of NO₂. For example, in the case of the daily temperature range, the number of subregions was four, and the average values of these subregions were 529.1566, 527.5779, 457.092, and 355.4332. The results for other factors were obtained, similarly. It is worth noting that the factor with the highest average NO₂ value could be identified as the major influencing factor [19]. The highest average value of each influencing factor was determined, and the results were shown in Fig. 5. The factors with the two largest average values were industrial smoke dust emissions and daily temperature range, with values of 552.3783 and 529.1566, respectively.

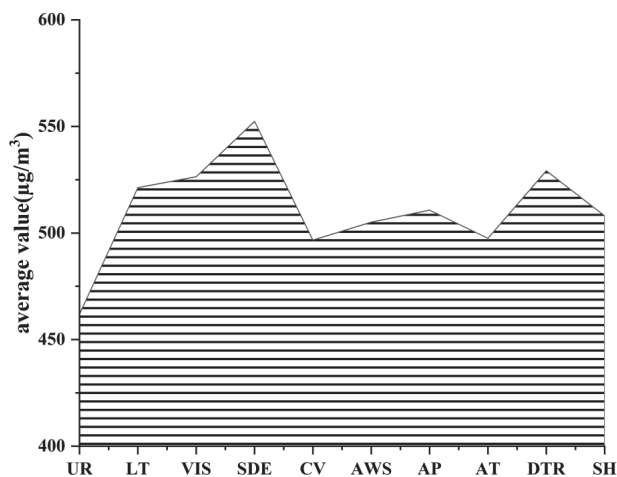


Fig. 5. The NO₂ average value of risk detection results.

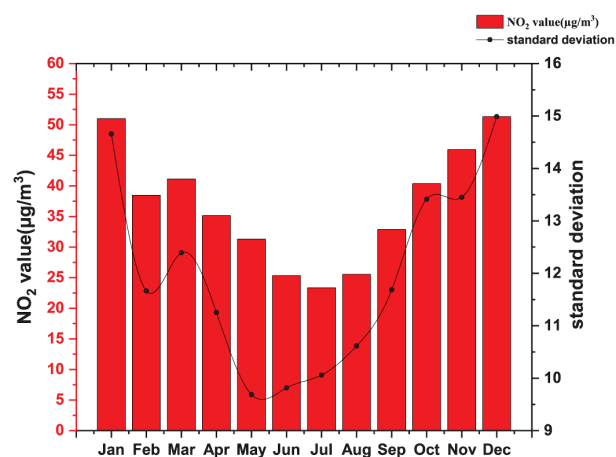


Fig. 7. Mean and standard deviation of monthly NO₂.

Annual Detection Results

The annual detection results were shown in Fig. 6. The annual mean q values were ranked in descending order as follows: industrial smoke dust emissions (0.358) > daily temperature range (0.349) > average precipitation (0.241) > urbanization rate (0.235) > increases in secondary industry (0.233) > average wind speed (0.203) > sunshine hours (0.193) > average temperature (0.145) > number of large trucks (0.088) > number of civilian vehicles (0.079). It could be concluded that industrial smoke dust emissions and daily temperature range were the two most important factors that determined the change in NO₂ concentration in each of the six years, and could reflect the spatial heterogeneity of NO₂.

Quarterly Detection Results

The monthly changes in NO₂ were illustrated in Fig. 7. Monthly changes in both the average and standard deviation of NO₂ concentration had a U-shaped variation trend, conforming to the findings of previous studies [20, 21]. Specifically, the highest NO₂ pollution level was observed in December, with a value of 51.34 µg/m³, while the corresponding lowest value of 23.34 µg/m³ was observed in July. To compare the seasonal changes in NO₂ concentration, the average value for each season was further calculated, and the mean values were listed in descending order as winter (46.93) > autumn (39.73) > spring (35.86) > summer (24.75), indicating that higher levels of NO₂ pollution occurred in winter and lower levels occurred in summer.

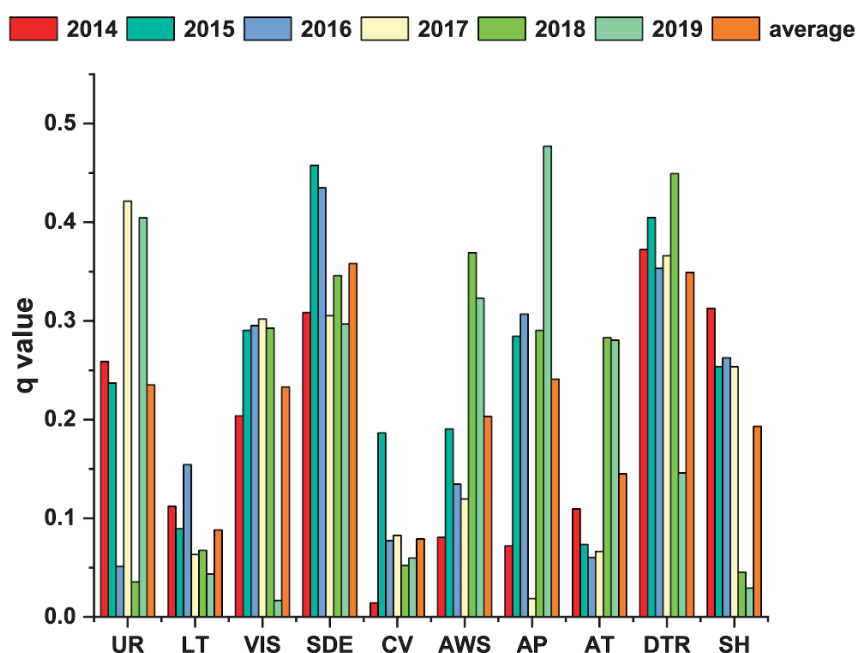


Fig. 6. Six-year average explanatory power.

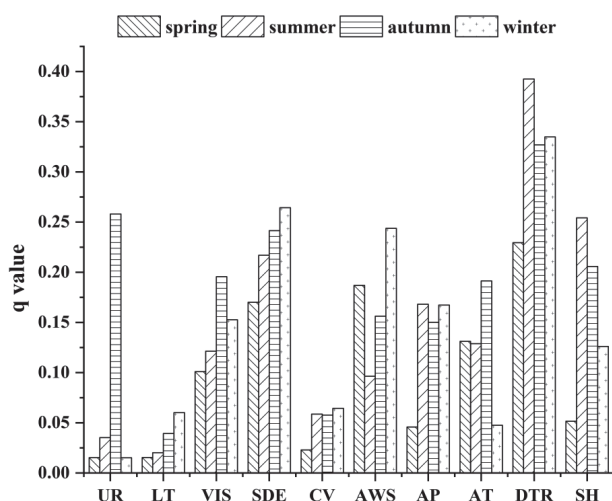


Fig. 8. Seasonal results for q value detection.

In all four seasons (Fig. 8), the influence of the daily temperature range was the strongest. Most of the influencing factors had the weakest effects on NO_2 in spring. The influence of sunshine hours was more notable in summer than in other seasons. The effects of urbanization rate were greater in autumn. The influence of industrial smoke dust emissions was more significant in winter.

Discussion

The main purpose of this study was to analyze the effects of selected influencing factors on the spatiotemporal distribution of NO_2 air pollution through geographical detection. The results showed that the daily temperature range was the most significant factor among meteorological factors whereas industrial smoke dust emissions had a greater influence than other anthropogenic factors. Moreover, according to the ecological detection results, the daily temperature range was significantly different from other factors except for industrial smoke dust emissions, which was why the daily temperature range and industrial smoke dust emissions had the two highest q values in the factor detection results; however, their interaction value was not the highest.

Spearman rank correlation analysis indicated positive associations between NO_2 concentration and industrial smoke dust emissions, daily temperature range, average precipitation, average temperature, number of large trucks and number of civilian vehicles, while sunshine hours, average wind speed, increases in secondary industry and urbanization rate all exerted a slight or moderate negative effect on NO_2 pollution, a finding that was consistent with many previous studies [22, 23]. These findings highlighted the significant role of meteorological and anthropogenic factors in the formation process of NO_2 pollution.

For instance, the number of large trucks and civilian vehicles are highly correlated with the intensity of human activity, resulting in increased fossil energy consumption and pollutant emissions; moreover, there is a relationship between aerosol content and daily temperature range because a decrease in aerosol content causes more solar radiation to reach the ground, increasing the daily temperature range [24].

It is worth noting that air quality in precipitation conditions is generally better than that in non-precipitation conditions because precipitation has an important scouring effect on air pollutants [25, 26]. A previous study found that precipitation was negatively correlated with air pollutants [27]. However, in this study, the correlation between precipitation and NO_2 was positive. The reason for this result could be explained by precipitation playing an important role in improving local air quality. However, it did not change the overall distribution pattern of air quality in Shandong Province.

Regarding the annual detection results, the influence of urbanization rate changed greatly because the regional development was unbalanced, and high spatial heterogeneity of urbanization was evident [28]. The q value of average precipitation in 2017 was by far the lowest among the six years. It was previously reported that according to the precipitation cycle in Shandong, 2014-2016 were dry years, with an average annual precipitation of 640 mm [29]; however, the annual precipitation began to increase in 2017, reaching 789.5 mm in 2018. Due to the extreme typhoon weather in central Shandong in 2018 and 2019, the influences of average wind speed and average temperature were stronger in these years. Sunshine hours had weaker influences in 2018 and 2019, which could be explained by the fact that sunshine hours have a high correlation with cloud cover [30], which reached maximum levels in 2018 and 2019 with values of 26% and 28%, respectively, strengthening the reflection and absorption of sunshine by the atmosphere and reducing the solar radiation reaching the ground. The environmental pollution caused by the rapid development of the petroleum industry and a lack of innovation have seriously restricted the economic transformation and sustainable development, and led to the great decrease in the influence of increases in secondary industry in 2019.

In terms of the seasonal patterns of air pollution, NO_2 pollution was more severe in spring and winter, which was similar to previous studies [31, 32]. Due to the increase in air pollutant emissions caused by heating in winter, the pollution in this season was higher [33]. On the other hand, the reduced levels of NO_2 pollution in summer could be attributed to the photochemical reaction of NO_2 being enhanced under the influence of solar radiation [34, 35].

Conclusions

This study was based on daily data from 2014 to 2019 comprising wind speed, temperature, and precipitation data from 91 monitoring stations in Shandong Province and data on other factors, including increases in secondary industry, daily temperature range, sunshine hours, urbanization rate, industrial smoke dust emissions, the number of large trucks and the number of civilian vehicles, which were analyzed using geographical detectors. We found that the daily temperature range and industrial smoke dust emissions were the two most important factors affecting the spatiotemporal distribution of NO₂ pollution. The pairwise interaction of these two factors enhanced their influence on the spatial and temporal characteristics of NO₂ pollution on the annual scale. NO₂ pollution had obvious seasonal variation; that is, the most severe pollution occurred in winter and the mildest pollution occurred in summer.

According to our findings, we should pay more attention to the influences of industrial smoke dust emissions and daily temperature range. Improving the emission reduction efficiency in the food manufacturing, chemical and other industries is the main way to reduce industrial smoke dust emissions. By controlling the contents of aerosols produced by human activity, the influence of daily temperature range on NO₂ pollution could be changed. Regarding the mutual enhancement effects of paired factors on NO₂ pollution, we can take corresponding measures, for instance, appropriately slowing the urbanization process to weaken its high interaction with increases in secondary industry. In terms of seasonal effects, we can make greater efforts to control the amount of coal burning and use clean energy to reduce air pollution in winter.

Acknowledgments

This work was supported by the National Natural Science Foundation of China (grant numbers 41771434 and 41930651) and the Fundamental Research Funds for the Central Universities (18CX02064A).

Conflicts of Interest

The authors declare that there is no conflict of interest regarding the publication of this paper.

References

1. WANG Z.H., ZHANG X., ZHOU Z.J., CHEN W.Y., ZHOU J.H., CEN K.F. Effect of Additive Agents on the Simultaneous Absorption of NO₂ and SO₂ in the Calcium Sulfite Slurry. *Energy & Fuels*, **26** (9), 5583, **2012**.
2. ZHANG Q.Q., PAN Y.P., HE Y.X., WALTERS WENDELL W., NI Q.Y., LIU X.Y., XU G.Y., SHAO J.L., JIANG C.L.

Substantial nitrogen oxides emission reduction from China due to COVID-19 and its impact on surface ozone and aerosol pollution. *Sci Total Environ*, **753** (7), 142238, **2021**.

3. KHAN A.A., JONG W.D., JANSENS P.J. Spliethoff H. Biomass combustion in fluidized bed boilers: Potential problems and remedies. *Fuel Process, Technol* **90** (1), 21, **2009**.
4. XIN Y., LI Q., ZHANG Z.L. Zeolitic Materials for DeNO_x Selective Catalytic Reduction. *ChemCatChem*, **10**, 29, **2018**.
5. SHAMS S.R., JAHANI A., KALANTARY S., MOEINADDINI M., KHORASANI N. Artificial intelligence accuracy assessment in NO₂ concentration forecasting of metropolises air. *Sci Rep*, **11**, 1805, **2021**.
6. AL-HEMOUD A., GASANA J., ALAJEEL A., ALHAMOUD E., AL-SHATTI A., AL-KHAYAT A. Ambient exposure of O₃ and NO₂ and associated health risk in Kuwait. *Environ Sci Pollut Res*, **28**, 14917, **2020**.
7. JIANG Q.T., CHRISTAKOS G. Space-time mapping of ground-level PM_{2.5} and NO₂ concentrations in heavily polluted northern China during winter using the Bayesian maximum entropy technique with satellite data. *Air Qual Atmos Health*, **11**, 23, **2017**.
8. MABAHWI N., LEH O., OMAR D. Human Health and Wellbeing: Human Health Effect of Air Pollution. *Procedia - Social and Behavioral Sciences*, **153**, 221, **2014**.
9. FRANCISCO P.W., JACOBS D.E., TARGOS L., DIXON S.L., BREYSSE J., ROSE W., CALI S. Ventilation. Indoor Air Quality, and Health in Homes Undergoing Weatherization. *Indoor Air*, **27**, 463, **2017**.
10. KHAMUTIAN R., NAJAFI F., SOLTANIAN M., SHOKOOHIZADEH M.J., POORHAGHIGHAT S., DARGAHI A., SHARAFI K., AFSHARI A. The association between air pollution and weather conditions with increase in the number of admissions of asthmatic patients in emergency wards: a case study in Kermanshah. *Med J Islam Repub Iran*, **29** (1), 558, **2015**.
11. HAN L.J., ZHOU W.Q., LI W.F. City as a major source area of fine particulate (PM_{2.5}) in China. *Environ Pollut*, **206**, 183, **2015**.
12. HAO Y., LIU Y.M. The influential factors of urban PM_{2.5} concentrations in China: a spatial econometric analysis. *J Clean Prod*, **112** (2), 1443, **2016**.
13. XIAO C.C., CHANG M., GUO P.K., GU M.F., LI Y. Analysis of air quality characteristics of Beijing-Tianjin-Hebei and its surrounding air pollution transport channel cities in China. *J Environ Sci*, **32** (1), 213, **2020**.
14. GUO H., WANG Y.G., ZHANG H.L. Characterization of criteria air pollutants in Beijing during 2014-2015. *Environ Res*, **154**, 334, **2017**.
15. LIU Z.H., WANG L.L., ZHU H.S. A time-scaling property of air pollution indices: a case study of Shanghai, China. *Atmospheric Pollution Research*, **6** (5), 886, **2015**.
16. HU J.L., WANG Y.G., YING Q., ZHANG H.L. Spatial and temporal variability of PM_{2.5} and PM₁₀ over the North China Plain and the Yangtze River Delta, China. *Atmos Environ*, **95**, 598, **2014**.
17. WANG J.F., XU C.D. Geodetector: Principle and Prospect. *Acta Geographica Sinica* **72** (1), 116, **2017** [In Chinese].
18. CHI Y., QIAN T.L., SHENG C.Y., XI C.B., WANG J.C. Analysis of Differences in the Spatial Distribution among Terrestrial Mammals Using Geodetector – A Case Study of China. *ISPRS Int. J. Geo-Inf*, **10** (1), 21, **2021**.
19. BAI L., JIANG L., YANG D.Y., LIU Y.B. Quantifying the spatial heterogeneity influences of natural and socioeconomic factors and their interactions on air

- pollution using the geographical detector method: A case study of the Yangtze River Economic Belt, China. *J Clean Prod*, **232**, 69, **2019**.
20. YU M.Y., XU Y.X., LI J.Q., LU X.C., XING H.Q., MA M.L. Geographic Detector-Based Spatiotemporal Variation and Influence Factors Analysis of PM_{2.5} in Shandong, China. *Pol.J.Environ.Stud*, **30** (1), 463, **2021**.
 21. ZHAN D.S., KWAN M.P., ZHANG W.Z., WANG S.J., YU J.H. Spatiotemporal Variations and Driving Factors of Air Pollution in China. *Int J Environ Res Public Health*, **14** (12), 1538, **2017**.
 22. ITO K., THURSTON G.D., SILVERMAN R.A. Characterization of PM_{2.5}, gaseous pollutants, and meteorological interactions in the context of time-series health effects models. *J. Expo. Sci. Environ. Epidemiol*, **17**, S45, **2007**.
 23. JIANG S., LONG R.Y., ZHAO K., LUO Z.G., CHEN C.W., LIU L.J. Air Pollution Characteristics and Cause Analysis of Main Urban Area of Western Guizhou in the Ghost Festival. *Meteorological and Environmental Research*, **12** (01), 26, **2021**.
 24. VOGEL B., VOGEL H., BÄUMER D., BANGERT M., LUNDGREN K., RINKE R., STANELLE T. The comprehensive model system COSMO-ART – Radiative impact of aerosol on the state of the atmosphere on the regional scale. *Atmospheric Chemistry and Physics*, **9** (22), 8661, **2009**.
 25. FUNG W.Y., WU R.G. Relationship between intraseasonal variations of air pollution and meteorological variables in Hong Kong. *Annals of GIS*, **20** (3), 217, **2014**.
 26. CHEN C., YU Z.B., XIANG L., HE J.J., FU X.L. Effects of Rainfall Intensity and Amount on the Transport of Total Nitrogen and Phosphorus in a Small Agricultural Watershed. *Applied Mechanics and Materials*, 212-213, 268–271, **2012**.
 27. WANG Y.Q., YANG X.L. The influence of precipitation situation in Harbin on the dilution of atmospheric pollutants. *Journal of Natural Disasters*, (05), 65, **2007** [In Chinese].
 28. DU X., FANG C.L., MA H.T. Coordination and temporal and spatial evolution of tourism economy and urbanization in coastal provinces: Taking Shandong Province as an example. *Economic Survey* **38** (01), 15, **2021** [In Chinese].
 29. DU Z.D., XIANG Z. Precipitation forecast and defense suggestions in the flood season in Shandong Province in 2019. *Shandong Water Resources* (08), 13, **2019** [In Chinese].
 30. LI Z.X., FENG Q., ZHANG W., HE Y.Q., WANG X.F., CATTO NORM., AN W.L., DU J.K., CHEN A.F., LIU L., HU M. Decreasing trend of sunshine hours and related driving forces in Southwestern China. *Theoretical and Applied Climatology*, **109** (1-2), 305, **2012**.
 31. LI Q., WANG E.R., ZHANG T.T., HU H. Spatial and Temporal Patterns of Air Pollution in Chinese Cities. *Water Air Soil Pollut*, **228**, 92, **2017**.
 32. MEGHDAD P., ABDOLLAH D., FATEME A., VAHIDEH F., FARNAZ A., FATEMEH N. The quality of air pollutant concentrations in Kermanshah emphasizing PM₁₀ due to the occurrence of dust (2011-2013). *Journal of Kermanshah University of Medical Sciences*, **18** (11), **2015**.
 33. ZHAN D.S., KWAN M.P., ZHANG W.Z., YU X.F., MENG B., LIU Q.Q. The driving factors of air quality index in China. *J Clean Prod*, **6**, 108, **2018**.
 34. CICHOWICZ R., WIELGOSIŃSKI G., FETTER W. Dispersion of atmospheric air pollution in summer and winter season. *Environ Monit Assess*, **189**, 605, **2017**.
 35. ESLAMI F., SALARI M., DEGHANI M. H., DARGAHI A., NAZMARA S., YAZDANI M., BEHESHTI A. Relationship of Formaldehyde Concentration in Ambient Air with CO, NO₂, O₃, Temperature and Humidity: Modeling by Response Surface Model. *Arch Hyg Sci*. **8** (1), 9, **2019**.